AJNR

MR imaging in radiation myelopathy.

P Y Wang, W C Shen and J S Jan

AJNR Am J Neuroradiol 1992, 13 (4) 1049-1055
http://www.ajnr.org/content/13/4/1049

MR Imaging in Radiation Myelopathy

Pao-Yu Wang,[1,4] Wu-Chung Shen,[2] and Jian-Sheng Jan[3]

Purpose: Using MR imaging, we assessed the signal, size, and enhancing characteristics of the cervical cord in patients in whom radiation myelopathy developed after radiotherapy for nasopharyngeal carcinoma. **Patients and Methods:** Ten patients, 3 men and 7 women, aged from 32 to 77 years, were included. MR imaging was performed 1 to 53 months after clinical manifestations of myelopathy. **Results:** Two cases showed atrophy of the cervical cord without abnormal signal intensity; in the others, a long segment of the cervical cord demonstrated low signal intensity on T1-weighted images and high signal intensity on T2- or T2*-weighted images. Some of these cases also showed swelling of the cord. Focal enhancement at C1-C2 area after intravenous administration of Gd-DTPA was seen in four cases. **Conclusions:** There is a correlation between the time of MR imaging after onset of symptoms and MR findings. When MR scans were obtained more than 3 years after onset of symptoms, atrophy of the cervical cord was noted without abnormal signal intensity. When MR was performed less than 8 months after onset of symptoms, a long segment of the cervical cord demonstrated abnormal signal intensity with or without associated swelling of the cord and focal enhancement.

Index terms: Spinal cord, magnetic resonance; Spinal cord, myelopathy; Therapeutic radiology, complications

AJNR 13:1049–1055, Jul/Aug 1992

Radiation myelopathy is a recognized complication of therapeutic irradiation (1–4). The clinical presentations are characterized by a subacute onset following a long asymptomatic period. Radiation myelopathy should be suspected when neurologic signs occur in the segment of an irradiated cord in patients with normal cerebrospinal fluid and no evidence of metastases. The myelogram is usually normal, but in cases of sharp clinical deterioration, myelography may show nonspecific, diffuse enlargement of the cord limited to the radiated field and the adjacent segment with or without block (5). The parenchymal changes of the cord in radiation myelopathy can easily be visualized with magnetic resonance (MR) imaging (6, 7). We studied the signal, size, and enhancing characteristics of the cervical cord in radiation myelopathy after radiotherapy of nasopharyngeal carcinoma (NPC).

Received June 11, 1991; accepted after revisions February 3, 1992.

Section of Neurology, Departments of [1] Internal Medicine, [2] Radiology, and [3] Radiation Oncology, Taichung Veterans General Hospital, Taichung, Taiwan, Republic of China.

[4] Address reprint requests to Pao-Yu Wang, MD, Section of Neurology, Department of Internal Medicine, Taichung Veterans General Hospital, No. 160, Section 3, Chung-Kang Road, Taichung, Taiwan, 40705, Republic of China.

AJNR 13:1049–1055, Jul/Aug 1992 0195-6108/92/1304–1049

Patients and Methods

A total of 10 consecutive patients presented with a radiation myelopathy, including two patients (cases 1 and 8) from a previous study (6). There were three men and seven women, aged from 32–77 years (median 42.5 years). All were diagnosed as NPC cases. Radiotherapy with a cobalt 60 unit was delivered in all, using a total of 70–84 Gy (median 71 Gy) in 35–42 fractions (median 35 fractions) to the nasopharynx and upper neck from bilateral opposing ports, and infraorbital ports or anterior port. The upper cervical cord (C1-C4) was estimated to have received a total of 40 Gy from the same ports, but the C1-C2 area in some patients might have received up to 64 Gy. The fractional dose was 2 Gy in every case. The lower neck received a total of 50–84 Gy in 25–42 fractions from anterior port, with central shielding to let the dose be delivered to the lower cervical cord (C5-C7) in less than 10 Gy. Case 7 developed radiation myelopathy 1 year after second radiotherapy to the recurrent NPC, with a total of 50 Gy in 25 fractions from bilateral ports and 11 Gy in 4 fractions by intracavitary brachytherapy (local nasopharyngeal irradiation with cobalt 60). Three cases (cases 2, 5, and 8) had received three courses of adjuvant chemother-

apy with cisplatin and 5-fluorouracil after completion of radiotherapy. Neurologic deficits confined to the medulla and/or the cervical cord developed after variable latent periods, ranging from 7–144 months (median 24.5 months). MR imaging was performed 1–53 months (median 2 months) after clinical manifestations. The criteria of tumor staging proposed by UICC (Union Internationale Contre le Cancer) 1988 were used. The patients were grouped into a shorter latent period if the latent periods were shorter than or up to 18 months and into a longer latent period if the latent periods were longer than 18 months. The staging of tumor, dosage of radiation to the nasopharynx and upper cervical cord, fractions, ports and port size, and chemotherapy are summarized in Table 1.

MR imaging was performed with a superconductive magnet operating at 1.0 T. In cases 1 and 8, spin-echo pulse sequence was used with parameters of 500–600/20/2–4 (TR/TE/excitations) for T1-weighted images, and 2000/30–100/2–4 for T2-weighted images. The section thickness was 4 mm in sagittal planes, and 6–7 mm in axial planes. In others, spin-echo pulse sequence was used with parameters of 500–550/20/2 for T1-weighted images, and gradient-echo pulse sequence was used with parameters of 400/18/4 and flip angle of 10° for T2*-weighted images. The section thickness was 4–4.5 mm in sagittal planes, and 4–6 mm in axial planes. Five cases (cases 2 and 4–7) were also studied with intravenous gadolinium diethylenetriamine pentaacetic acid (Gd-DTPA) injection. Case 6 had a second MR imaging 3 months after the first.

Results

In the shorter latency group, low signal intensity on T1-weighted images and high signal intensity on T2- or T2*-weighted images with swelling of the cord in a long segment of the cervical cord were seen in cases 1 and 2. Intravenous Gd-DTPA injection showed focal contrast enhancement in the central and left lateral cord at C1-C2 level in case 2. Atrophy of the cervical cord at C1-C2 level without abnormal signal intensity was seen in case 3 (Fig. 1).

In the longer latency group, low signal intensity on T1-weighted images and high signal intensity on T2- or T2*-weighted images in a long segment of the cervical cord with swelling of the cord were seen in cases 4, 6, 7, and 9, and without swelling of the cord in cases 5 and 8. Intravenous Gd-DTPA injection showed no contrast enhancement in case 7, focal contrast enhancement in the central and left lateral cord at C1-C2 level in case 4 (Fig. 2), and in the central and right lateral cord in cases 5 and 6 (Fig. 3). The latent periods, time of MR imaging after onset of symptoms, clinical manifestations, MR findings, enhancement patterns, and clinical follow-up are summarized in Table 2.

TABLE 1: Summary of radiotherapeutic profiles in 10 cases of radiation myelopathy after radiotherapy of nasopharyngeal carcinoma

Case No.	Sex/Age (year)	Tumor Staging	Total Dose[a] to Nasopharynx	Fractions	Port and Port Size (cm)	Estimated Dose[a] to Cervical Cord	Chemotherapy
Shorter latent period							
1	F/50	T4N2M0	70	35	Bilateral Infraorbital	?	–
2	M/39	T4N3bM0	74	37	Bilateral (14 × 12) Anterior (6 × 7)	40–64	+
3	F/34	?	84	42	Bilateral Anterior	44–61.5	–
Longer latent period							
4	F/65	T2N3aM0	70	35	Bilateral (13 × 11) Infraorbital (6 × 6)	40–65	–
5	M/40	T4N3bM0	74	37	Bilateral (15 × 11.5) Anterior (8 × 8)	40–64	+
6	F/45	T2N1M0	70	35	Bilateral (14 × 12) Infraorbital (6 × 6)	40–60	–
7	F/32	T2N3aM0	72	36	Bilateral (12 × 10) Infraorbital (5 × 5)	40–62	–
			60[b]	30	Bilateral (6 × 5)	10	–
8	M/36	T3N3bM0	75	37	Bilateral (15 × 12) Anterior (6 × 6)	45	+
9	F/77	T2N0M0	70	35	Bilateral (12 × 10) Infraorbital (6 × 6)	40–60	–
10	F/57	?	70	35	Bilateral (9 × 7) Oblique (4 × 5)	?	–

[a] Dose in Gy.

[b] Second radiotherapy 2 years after the first.

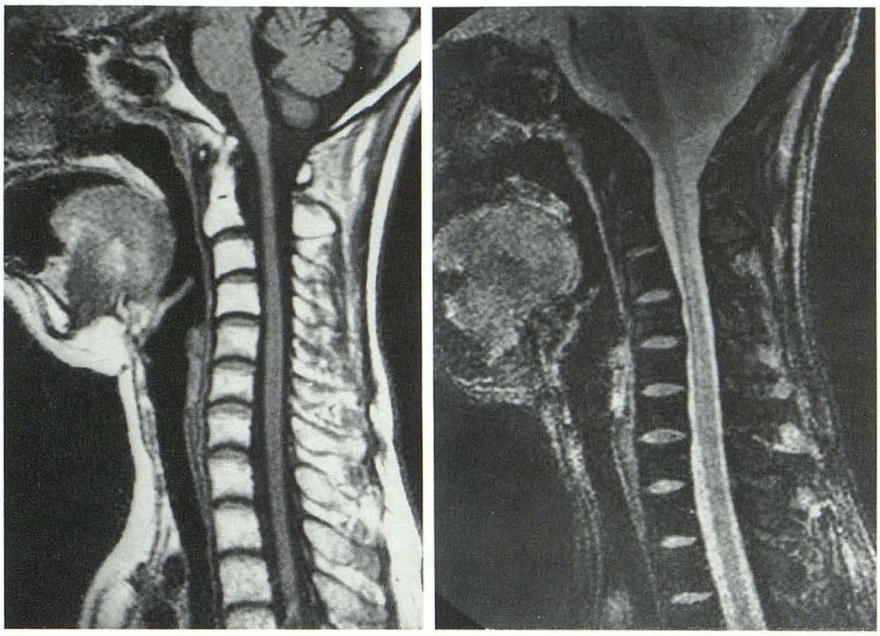

A B

Fig. 1. MR images of the cervical cord in case 3.

A, Sagittal T1-weighted spin-echo images, 550/20/2 and section thickness of 4.5 mm, show atrophy of the cervical cord at C1-C2 level. Diffuse increased signal intensity of the vertebrae due to fatty replacement of marrow secondary to radiation is also seen.

B, Sagittal T2*-weighted gradient-echo images, 400/18/4 and section thickness of 4.5 mm, show no abnormal signal changes.

Discussion

There were only a few case reports on the MR findings of radiation myelopathy (6, 7). The signal, size, and enhancing characteristics of the cord in radiation myelopathy on MR imaging are unknown. The relationship between the MR findings and latent periods of radiation myelopathy is uncertain. Our study shows no correlation between the MR findings and latent periods. Instead, there is a correlation between the time of MR imaging after onset of symptoms and MR findings. When the time of MR imaging after onset of symptoms is shorter than 8 months, MR images show low signal intensity on T1-weighted images and high signal intensity on T2- or T2*-weighted images in a long segment of the cervical cord. Swelling of the cord or focal enhancement after intravenous Gd-DTPA injection may be associated. These abnormal MR findings may persist for variable periods of at least several months. When the time of MR imaging after onset of symptoms is longer than 3 years, atrophy of the cervical cord without abnormal signal intensity is noted.

The standard treatment of NPC in our hospital is radiotherapy delivered via a cobalt 60 unit. The daily fractional dose is 2 Gy administered to the nasopharynx. Bilateral opposing ports with port size varied from 12–15 cm × 10–12 cm to encompass the basal skull and upper neck are used first. The dose from bilateral ports is 40 Gy in 20 fractions. Then infraorbital ports, with sizes ranging from 5 × 5 cm to 6 × 6 cm in order to encompass the nasopharynx, are used with a dose of 30 Gy in 15 fractions. Booster doses may be given for larger tumors from bilateral small ports. Some patients may be treated with an anterior central port in place of the infraorbital ports for the tumor with anterior involvement. The upper cervical cord (C1-C4) is estimated to receive a total of 40 Gy from bilateral opposing ports. The medulla oblongata and C1 of the cervical cord may receive 0.5–2.5 Gy from infraorbital ports or anterior port. The upper neck may receive booster treatment with an anterior port by central shielding or with 7–9 MeV electron beams. The dose delivered to the upper cervical cord from booster treatment is negligible. The lower neck is irradiated with 50–70 Gy in 25–35 fractions from an anterior single port with a central 3–4 cm block shielding. The dose to the lower cervical cord is estimated to be less than 10 Gy.

The incidence of radiation myelopathy correlates positively with the total radiation dose, dose per fraction, and length of the spinal cord irradiated. The incidence of radiation myelopathy after radiotherapy for NPC is estimated to be 1%–10% (1, 8, 9). Although a valid statistical dose-response curve has still not been established, estimates of the conventionally fractionated dose causing a 5% and 50% incidence of radiation myelopathy are 57–61 Gy and 68–73 Gy, respectively (10–12). The latent periods of radiation

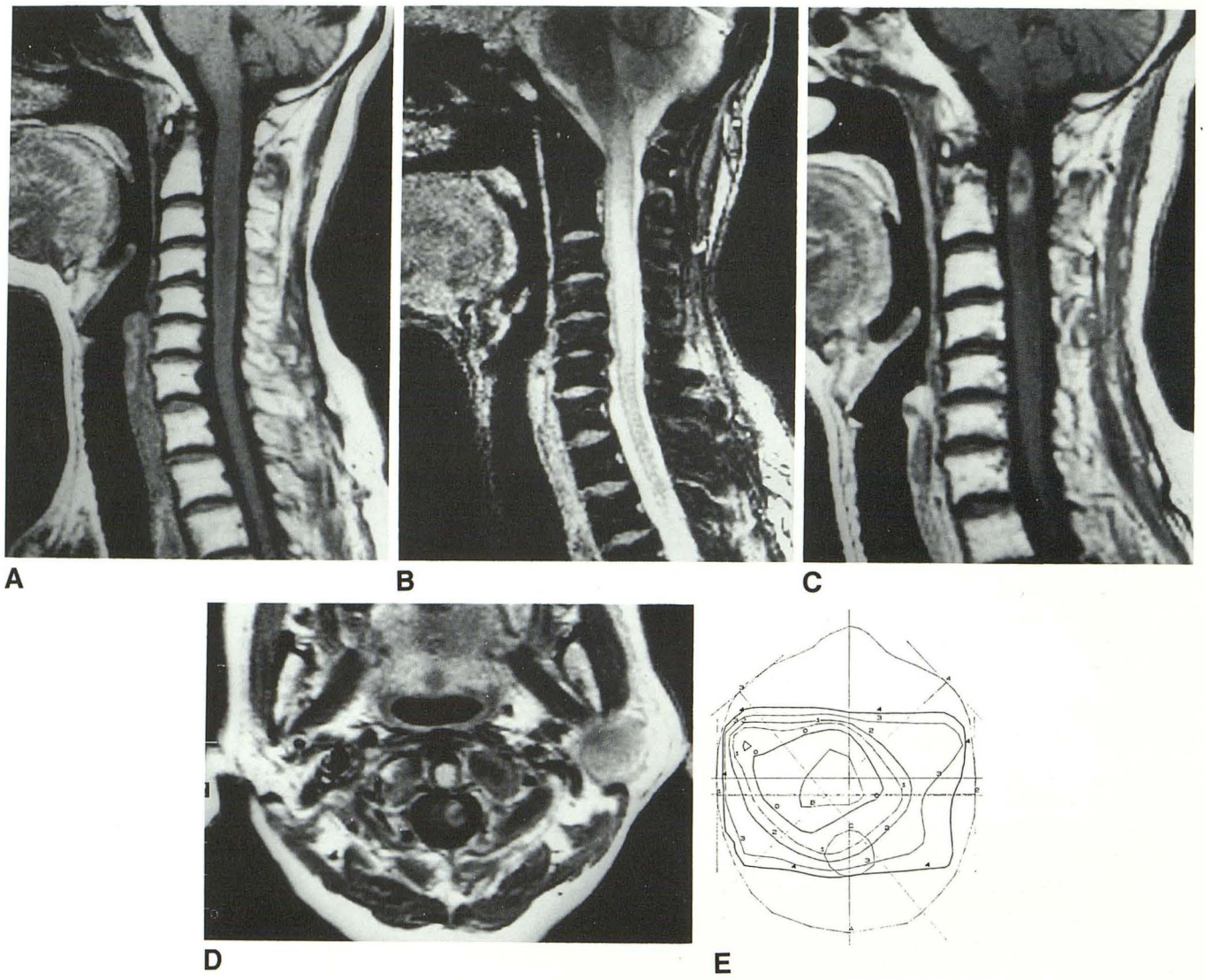

Fig. 2. MR images of the cervical cord and isodose curve in case 4.

A, Sagittal T1-weighted spin-echo images, 500/20/2 and section thickness of 4 mm, show low signal intensity and swelling of the cord from C1-C6. Diffuse increased signal intensity of the vertebrae due to fatty replacement of marrow secondary to radiation is also seen.

B, Sagittal T2*-weighted gradient-echo images, 400/18/4 and section thickness of 4 mm, show increased signal intensity in previous low signal area in *A*.

C and *D*, Sagittal and axial T1-weighted spin-echo images, 500/20/2 and section thickness of 4 mm in sagittal planes and 6 mm in axial planes, with intravenous Gd-DTPA injection show focal enhancement at C1-C2 (*C*) and eccentric toward the left (*D*).

E, Isodose curve of case 4. Areas of isodose are indicated as follows: 0:70 Gy, 1:65 Gy, 2:60 Gy, 3:50 Gy, 4:40 Gy. Area *B* indicates the contour of the tumor and area *C* indicates the contour of the cervical cord of C1-C2 level.

myelopathy are bimodally distributed with two distinct peaks at 12–14 months and 24–28 months, and the latent periods decrease with an increasing dose (13). The histopathology of radiation myelopathy are classified as primarily white matter parenchymal lesions (type 1), primarily vascular lesions (type 2), or a combination of vascular and white matter lesions (type 3) (14). The white matter lesions and the combination of vascular and white matter lesions have the shorter latent periods corresponding to the earlier peak at 12–14 months, whereas the vascular lesions are associated with the longer latent periods corresponding to the second peak at 24–28 months. Although there is a correlation between the latent periods and histopathologic changes of radiation myelopathy (13, 14), no correlation between the MR findings and latent periods was found in our study.

Radiation myelopathy of the thoracic cord in the rabbit model with a radiation dose of 30 Gy showed a geographically distinct region of abnor-

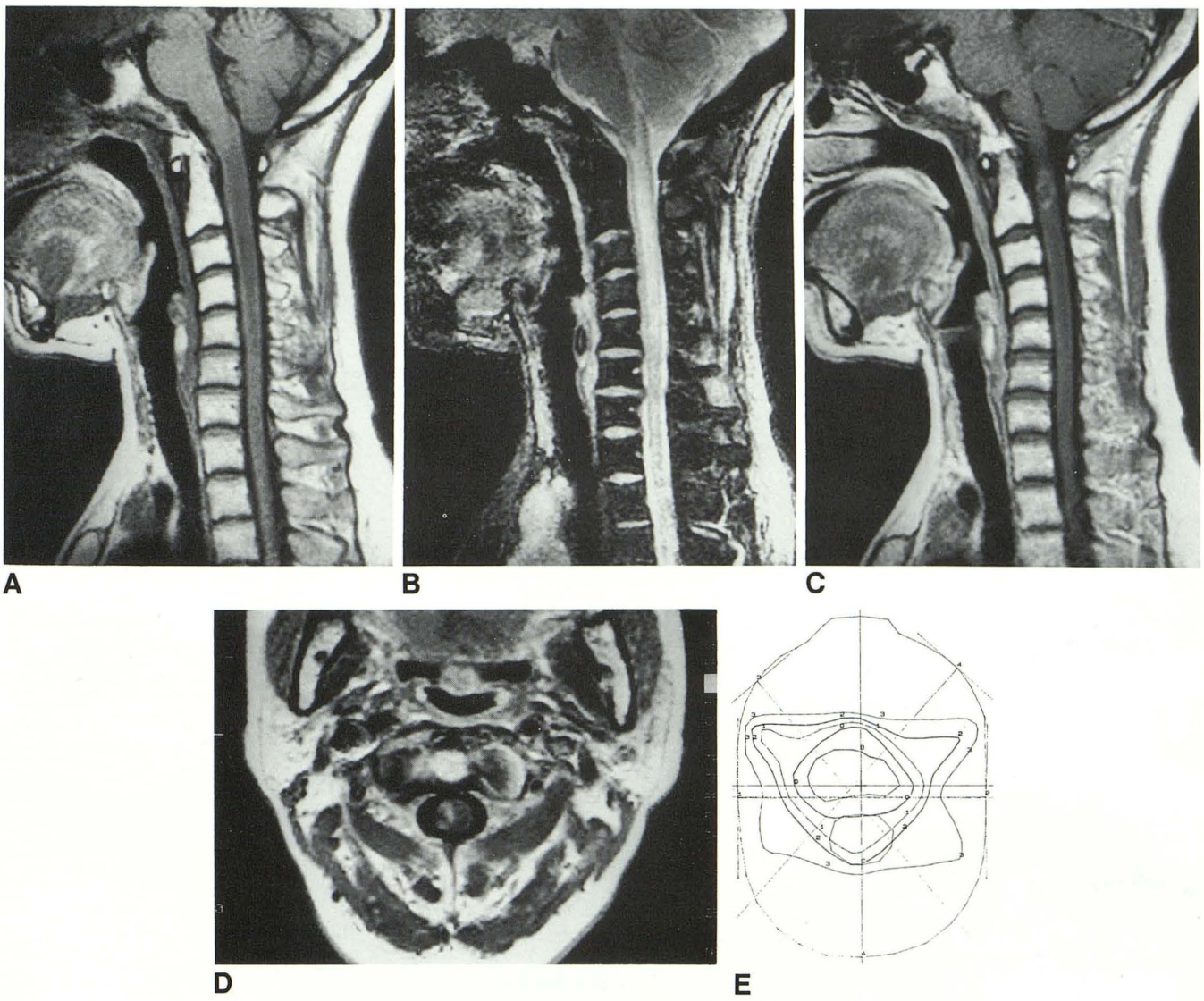

Fig. 3. The first MR images of the cervical cord and isodose curve in case 6.

A, Sagittal T1-weighted spin-echo images, 500/20/2 and section thickness of 4 mm, show low signal intensity and swelling of the cord from C1-C5. Diffuse increased signal intensity of the vertebrae due to fatty replacement of marrow secondary to radiation is also seen.

B, Sagittal T2*-weighted gradient-echo images, 400/18/4 and section thickness of 4 mm, show increased signal intensity in previous low signal area in *A*.

C and *D*, Sagittal and axial T1-weighted spin-echo images, 500/20/2 and section thickness of 4 mm in sagittal and axial planes, with intravenous Gd-DTPA show focal enhancement at C1-C2 (*C*) and eccentric toward the right (*D*).

E, Isodose curve of case 6. Areas of isodose are indicated as follows: 0:70 Gy, 1:65 Gy, 2:60 Gy, 3:50 Gy. Area *B* indicates the contour of the tumor and area *C* indicates the contour of the cervical cord of C1-C2 level.

mal high signal intensity on MR images, corresponding to the irradiated segment of spinal cord (15). The histopathology showed demyelination, focal astrocytosis, erythrodiapedesis, and perineuronal edema in the irradiated cord. The MR lesion was recognized prior to or with the onset of radiation myelopathy, but it is not known how early the MR lesion appears and how the MR lesion changes.

Zweig et al (7) reported the MR findings of a histologically confirmed case of radiation myelopathy. This patient received 5580 cGy in 31 fractions to the posterior fossa, and 2520 cGy at 180 cGy/fraction to the cervical and thoracic spine after resection of medulloblastoma of the left cerebellar hemisphere. Twenty months later, the patient developed progressive right-sided weakness and paresthesia beginning in the lower extremity and progressing to involve the upper extremity. MR imaging showed abnormal high

TABLE 2: Summary of clinical profiles and MR findings in 10 cases of radiation myelopathy after radiotherapy of nasopharyngeal carcinoma

Case No.	Latent Period	Time of Imaging[a]	Clinical Manifestations	MR Findings	Contrast Study	Clinical Follow-up
Shorter latent period						
1	7 mo	8 mo	Left BSS	Low signal intensity on T1WI, high signal intensity on T2WI, swelling of the cervical cord from C1-C6	ND	Recurrence, loss of follow-up
2	15 mo	2 mo	Left BSS	Low signal intensity on T1WI, high signal intensity on T2*WI, swelling of the cervical cord from C1-C6	Focal enhancement at C1-C2	Dead 5 mo after onset
3	18 mo	53 mo	Right BSS	Atrophy of the cervical cord at C1-C2 on T1 and T2*WI	ND	Recurrence, dead 63 mo after onset
Longer latent period						
4	22 mo	1 mo	Left BSS	Low signal intensity on T1WI, high signal intensity on T2*WI, swelling of the cervical cord from C1-C6	Focal enhancement at C1-C2	Worsening
5	23 mo	1 mo	Right BSS	Low signal intensity on T1WI, high signal intensity on T2*WI from C1-C5	Focal enhancement at C1-C2	Bone metastases, dead 5 mo after onset
6	26 mo	2 mo	Right BSS	Low signal intensity on T1WI, high signal intensity on T2*WI, swelling of the cervical cord from C1-C5	Focal enhancement at C1-C2	Dead 6 mo after onset
		5 mo		Same as above	Same as above	
7	36 mo	6 mo	Right HP	Low signal intensity on T1WI, high signal intensity on T2*WI, swelling of the cervical cord from C1-T1	No enhancement	Recurrence, loss of follow-up
8	48 mo	1 mo	Left BSS and BP	Low signal intensity on T1WI, high signal intensity on T2WI in the medulla and high cervical cord	ND	Bone metastases, dead 6 mo after onset
9	50 mo	2 mo	Right BSS	Low signal intensity of T1WI, high signal intensity on T2*WI, swelling of the medulla and upper cervical cord to C4	ND	Stationary
10	144 mo	36 mo	QP	Diffuse atrophy of the cervical cord	ND	Stationary

Note.—Abbreviations: BSS, Brown-Séquard syndrome; HP, hemiparesis; BP, bulbar palsy; QP, quadriparesis; ND, not done.

[a] Time of imaging after onset.

signal intensity from medulla to C5 level on T2-weighted images and focal ovoid area of contrast enhancement within the central and right lateral cord at the C1-C2 level. The biopsy of the region of focal enhancement showed mild vacuolation and minimal gliosis of the white matter with fibrinoid damage of small vessels and capillaries, consistent with the pathology of radiation changes. Whether any pathologic differences exist in areas of cord exhibiting T2 prolongation without contrast enhancement is unclear.

The MR findings of cases 2, 4, 5, and 6 were similar to that reported by Zweig et al. The laterality of focal enhancement correlated well with the side of weakness. The pathophysiologic mechanisms for focal contrast enhancement all in the upper cervical cord are uncertain, but is presumably due to the high radiation doses to

that area and attributed to the close proximity of the C1-C2 area to the nasopharynx or vascular factors, such as venous drainage.

In conclusion, a correlation between the time of MR imaging after onset of symptoms and MR findings is found in our study. When MR scan was performed more than 3 years after onset of symptoms, atrophy of the cervical cord was noted without abnormal signal intensity. When MR scan was performed less than 8 months after onset of symptoms, a long segment of the cervical cord demonstrated abnormal signal intensity with or without associated swelling of the cord and focal contrast enhancement.

References

1. Hung TP. Myelopathy following radiotherapy of nasopharyngeal carcinoma. *Proc Aust Assoc Neurol* 1968;5:421–428
2. Reagan TJ, Thomas JE, Colby MY. Chronic progressive radiation myelopathy, its clinical aspects and differential diagnosis. *JAMA* 1968;202:128–132
3. Jellinger K, Sturm KW. Delayed radiation myelopathy in man: report of twelve necropsy cases. *J Neurol Sci* 1971;14:389–408
4. Palmer JJ. Radiation myelopathy. *Brain* 1972;95:109–122
5. Shapiro R. *Myelography*. 4th ed. Chicago: Year Book, 1984: 289–292
6. Wang PY, Shen WC. Magnetic resonance imaging in two patients with radiation myelopathy. *J Formosan Med Assoc* 1991;90: 583–585
7. Zweig G, Russell EJ. Radiation myelopathy of the cervical spinal cord: MR findings. *AJNR* 1990;11:1188–1190
8. Tokars RP, Griem ML. Carcinoma of the nasopharynx an optimization of radiotherapeutic management for tumor control and spinal cord injury. *Int J Radiat Oncol Biol Phys* 1979;5:1741–1748
9. Mesic JB, Fletcher GH, Goepfert H. Megavoltage irradiation of epithelial tumors of the nasopharynx. *Int J Radiat Oncol Biol Phys* 1981; 7:447–453
10. McCunniff AJ, Liang MJ. Radiation tolerance of the cervical spinal cord. *Int J Radiat Oncol Biol Phys* 1989;16:675–678
11. Marcus RB, Million RR. The incidence of myelitis after irradiation of the cervical spinal cord. *Int J Radiat Oncol Biol Phys* 1990;19:3–8
12. Schultheiss TE. Spinal cord radiation tolerance: doctrine versus data. *Int J Radiat Oncol Biol Phys* 1990;19:219–221
13. Schultheiss TE, Higgins EM, El-Mahdi AM. The latent period in clinical radiation myelopathy. *Int J Radiat Oncol Biol Phys* 1984;10: 1109–1115
14. Schultheiss TE, Stephens LC, Maor MH. Analysis of the histopathology of radiation myelopathy. *Int J Radiat Oncol Biol Phys* 1988;14: 27–32
15. Rubin P, Whitaker JN, Ceckler TL, et al. Myelin basic protein and magnetic resonance imaging for diagnosing radiation myelopathy. *Int J Radiat Oncol Biol Phys* 1988;15:1371–1381

Please see the Commentary by Schultheiss on page 1056 in this issue.